

An Improved Finite Element Model for Thermal Balance Analysis of Aluminum Electrolysis Cells

Cui Xifeng, Zhou Yiwen, Yang Jianhong
 Green Metallurgy&Materials Division, Zhengzhou Research Institute of CHALCO, Zhengzhou, Henan, 450041, P.R. China

Keywords: Aluminum cells, Thermal balance analysis, thermal-electric coupling, Finite element model

Abstract

Thermal balance analysis, through which the insulation construction and daily operations of aluminum cells can be determined to keep electrolysis temperature stable, is of capital importance for the cell design. This paper propose an improved thermal-electric coupling model based on finite element software ANSYS for thermal balance analysis. Besides ohmic heating effect and heat dissipation outside the cell, the model also takes into consideration the thermal effect caused by tapping, spent anode removal, fume/air extraction and raw materials heating. The numerical model is applied to a 305kA cell and is verified by comparing results with industrial measurements.

Introduction

Aluminum reduction cell is the key equipment in aluminium smelting process. It is not only a container for the electrochemical reaction, but also an electro-heater that generates Joule heat with the input current. The Joule heat sustains high melt temperature for the electrochemical reactions and normal operations. A rational thermal design of the aluminium cell is the one that hold electric thermal balance, then well-shaped ledge profile, low horizontal current component and finally high current efficiency is achieved.

Since the Hall-Herout electrolysis process was discovered more than one century ago, researchers around the world has done a lot of work about the side ledge formation [1-3], thermal insulation design [4-5] and thermal balance [6-7]. There are three thermal transfer ways inside and around electrolytic tank, including heat conduction, convection and radiation. In addition, the cell structure with many construction materials of different properties and shapes is intricate, and there are a variety of heat effects covering Joule heat, chemical reaction heat, heat dissipation, heat loss caused by anode change, fume/air extraction and taping, and so on. As a result, it is difficult to determine the temperature distribution of aluminium electrolysis cell.

As early as 1971, Haupin [8] proposed a 1D heat flow model for the calculation of freeze thickness. Kryukovsky[9] also calculated the temperature profile using a 1D thermal model. Since then, with the development of computational software and hardware technology, 2D and 3D thermal-electric coupled models are gradually available [6,10]. Gennady V. Arkhipov [4] presented a 3D thermal-electric model to calculate thermal and electric fields with account of raw materials heating energy and detailed electrochemical effect. Similarly, this paper proposes a quarter 3D thermal-electric model to calculate thermal balance during aluminium electrolysis process. Apart from Joule heat, the influence of daily operations is also considered. All the electrochemical reactions directly affect current efficiency, so the thermal effect caused by the decreased CE is introduced to the 3D model.

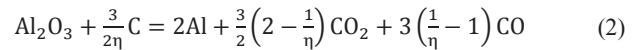
Thermal balance calculation

For an optimum cell design, holding heat balance is critical for minimizing energy consumption and promoting ease of operation. It should maintain exactly the temperature necessary for the electrolysis, and the heat flow should be sufficient enough to keep a well-shaped layer of frozen electrolyte over the side wall for protection. The whole cell is taken as a calculation system in order to calculate the cell's thermal balance. The voltage drop of the system is defined as follows:

$$V_{total} = V_a + V_g + V_b + V_c + V_{con} + V_{dec} + V_p \quad (1)$$

Where, V_a , V_g , V_b and V_c are the ohmic voltage drop of anode, gas layer, bath and cathode respectively; V_{con} is the contact voltage drop between cathode carbon and steel bar; V_{dec} is the decomposition voltage, 1.2 V for the electrode reaction with prebaked carbon anode; and V_p is the polarization voltage, about 0.25-0.45 V here.

For the carbon anode, the following material balanced equation of the cell reaction is obtained,



Where, η is the current efficiency, if CE is 90%, then $\eta=0.9$.

Energy input

Taking the ambient temperature 30°C as base temperature or reference temperature for thermal balance calculation, the energy input is described as

$$A_{total} = A_{ele} + A_{mat}^{t_1-30} \quad (3)$$

(1) Energy from electric power supply A_{ele}

$$A_{ele} = I \times V_{total} \text{ (W)} \\ = I \times (V_a + V_g + V_b + V_c + V_{con}) + I \times V_{dec} + I \times V_p \text{ (W)} \quad (4)$$

Where, I is the amperage of the aluminium reduction cell, A.

(2) Energy from raw materials $A_{mat}^{t_1-30}$

Prior to reaction (2), the carbon and alumina should be appropriate prepared. For every 2 mol (54 g) of aluminium production, 1 mol of alumina and $\frac{3}{2\eta}$ mol of carbon are required. As a result, the energy from alumina and carbon per kilogram aluminium is expressed as

$$(\Delta H_T^\circ)_{mat}^{t_1-30} = \left[(\Delta H_T^\circ)_{Al_2O_3}^{t_1-30} + \frac{3}{2\eta} (\Delta H_T^\circ)_C^{t_1-30} \right]$$

$$\times \frac{1000}{54} [\text{kJ} \cdot (\text{kgAl})^{-1}] \quad (5)$$

Where, $(\Delta H_T^\circ)_{mat}^{t_1-30}$ is the energy change of raw materials per kilogram aluminium from t_1 to 30°C, $\text{kJ} \cdot (\text{kgAl})^{-1}$; $(\Delta H_T^\circ)_{Al_2O_3}^{t_1-30}$ and $(\Delta H_T^\circ)_C^{t_1-30}$ are enthalpy change per mole of alumina and carbon, respectively, from t_1 to 30°C, $\text{kJ} \cdot \text{mol}^{-1}$.

In one hour, $0.33561 \eta \times 10^{-3} \text{ kg Al}$ is produced. Then in one second time, $A_{mat}^{t_1-30}$ for the whole calculation system is

$$A_{mat}^{t_1-30} = (\Delta H_T^\circ)_{mat}^{t_1-30} \times \frac{0.33561 \eta \times 10^{-3}}{3600} \text{ (kW)} \quad (6)$$

The raw materials enter pots at workshop temperature, $t_1 = 30^\circ\text{C}$, so $A_{mat}^{t_1-30}$ is 0 kW.

Energy expenditure

Total energy input A_{total} should be equal to total energy expenditure Q_{total} so as to reach thermal equilibrium. The energy expenditure is divided into the following items.

$$Q_{total} = Q_{dec} + Q_{alu} + Q_{and} + Q_{gas} + Q_{loss} \quad (7)$$

(1) Energy for decomposition reaction Q_{dec}

Decomposition reaction is showed as formula (2). According to first law of thermodynamics and related thermodynamic manual, the theoretical minimum energy required to produce 1 kg of Al could be calculated as:

$$\begin{aligned} \Delta H_T^\circ &= \left[\frac{3}{2} \left(2 - \frac{1}{\eta} \right) (\Delta H_T^\circ)_{CO_2} + 3 \left(\frac{1}{\eta} - 1 \right) (\Delta H_T^\circ)_{CO} - \right. \\ &\quad \left. (\Delta H_T^\circ)_{Al_2O_3} \right] \times \frac{1000}{54} [\text{kJ} \cdot (\text{kgAl})^{-1}] \\ &= \left(842.38 + 251.97 \times \frac{1}{\eta} \right) \times \frac{1000}{54} [\text{kJ} \cdot (\text{kgAl})^{-1}] \\ &= \left(15.60 + \frac{4.67}{\eta} \right) \times 10^3 [\text{kJ} \cdot (\text{kgAl})^{-1}] \end{aligned} \quad (8)$$

Where, $(\Delta H_T^\circ)_{CO_2}$, $(\Delta H_T^\circ)_{CO}$ and $(\Delta H_T^\circ)_{Al_2O_3}$ are the formation heat of CO_2 , CO and Al_2O_3 respectively, $\text{kJ} \cdot \text{mol}^{-1}$.

In one second time, Q_{dec} for the whole calculation system could be obtained as:

$$\begin{aligned} Q_{dec} &= \frac{0.33561 \eta \times 10^{-3}}{3600} \times \left(15.60 + \frac{4.67}{\eta} \right) \times 10^3 \text{ kJ} \cdot \text{s}^{-1} \\ &= (1.454 \eta + 0.435) \times 10^{-3} \text{ (kW)} \end{aligned} \quad (9)$$

(2) Energy taken away with removed liquid aluminium $Q_{alu}^{t_2-30}$

After reaction (2), aluminium is produced and siphoned away at electrolysis temperature (t_2). In one second time, Q_{alu} for the whole calculation system is

$$Q_{dec} = \frac{0.33561 \eta \times 10^{-3}}{3600} \times \frac{(\Delta H_T^\circ)_{alu}^{t_2-30}}{27} \text{ (kW)} \quad (10)$$

Where, $(\Delta H_T^\circ)_{alu}^{t_2-30}$ is enthalpy change of aluminium from t_2 to 30°C, $\text{kJ} \cdot \text{mol}^{-1}$; $t_2 = 950^\circ\text{C}$.

(3) Heat losses caused by anode change Q_{and}

The carbon anodes are consumable, so they should be replaced at regular intervals. According to formula (2), the net consumption of carbon is

$$m_{c,net} = \frac{0.33561 \eta \times 10^{-3}}{3600 \times 54} \times \frac{3}{2 \eta} \times 12 \text{ (kg} \cdot \text{s}^{-1}) \quad (11)$$

The gross consumption of anode carbon includes actual consumption and removed butts. It is described as:

$$m_{c,gross} = \frac{M_{and}}{TIME} \text{ (kg} \cdot \text{s}^{-1}) \quad (12)$$

Where, $m_{c,gross}$ is gross consumption of anode carbon, $\text{kg} \cdot \text{s}^{-1}$; M_{and} is total mass of carbon for one anode, kg; $TIME$ is average time interval between two anode changing operation, s.

So the quantity of removed butts (m_{butts}) is described as:

$$m_{butts} = m_{c,gross} - m_{c,net} \quad (13)$$

The quantity of removed anode steel claw (m_{claw}) is got as:

$$m_{claw} = \frac{M_{claw}}{TIME} \text{ (kg} \cdot \text{s}^{-1}) \quad (14)$$

Where, M_{claw} is total mass of steel claw of one anode, kg.

Energy taken away with removed anode (Q_{and}^1) is obtained:

$$Q_{and}^1 = m_{butts} \times (\Delta H_T^\circ)_c^{t_c-30} + m_{claw} \times (\Delta H_T^\circ)_{steel}^{t_{steel}-30} \quad (15)$$

Where, t_c is temperature of butts and t_{steel} is temperature of steel, they were measured before anode changing, °C; $(\Delta H_T^\circ)_c^{t_c-30}$ is enthalpy change of carbon from t_c to 30 °C, $\text{kJ} \cdot \text{mol}^{-1}$; $(\Delta H_T^\circ)_{steel}^{t_{steel}-30}$ is enthalpy change of steel from t_{steel} to 30°C, $\text{kJ} \cdot \text{mol}^{-1}$.

In anode changing process, the steel hood up the cell is locally removed. Even the anode cover is pushed aside until the operation is finished. Therefore, a lot of heat is dissipated during the period. The missing heat (Q_{and}^2) is calculated by formula (16).

$$Q_{and}^2 = n \alpha A (t_c - 30) \times \frac{time}{TIME} \quad (16)$$

Where, A is the area of one top steel hood, m^2 ; n is the number of removed hood; α is the heat transfer coefficient between top anode and environment, $\text{W} \cdot \text{m}^{-2} \cdot ^\circ\text{C}$. $time$ is duration time of anode changing process, s.

Therefore the total heat loss caused by anode change is

$$Q_{and} = Q_{and}^1 + Q_{and}^2 \quad (17)$$

(4) Energy taken away with fume/air gases Q_{gas}

The high temperature fume/air gases are sucked away from aluminium cell to gas scrubber then released to surrounding atmosphere by the cell ventilation. Q_{gas} is directly determined by

the gases suction rate, which has a strong impact on the duct gas temperature and gas emission rate. Through the measurement of the duct gas temperature and gas emission rate by flue gas analyzer, Q_{gas} could be figured out.

$$Q_{\text{gas}} = (\Delta H_T^\circ)_{m,\text{gas}/\text{fume}}^{t_3-30} \rho V \quad (\text{kW}) \quad (18)$$

Where, t_3 is temperature of gas/fume when they are emitted from cell, °C; $(\Delta H_T^\circ)_{m,\text{gas}/\text{fume}}^{t_3-30}$ is enthalpy change of gas/fume from t_3 to environment 30°C, $\text{kJ} \cdot \text{kg}^{-1}$; ρ is density of gas/fume, $\text{kg} \cdot \text{m}^{-3}$; V is volume flow rate of gas/fume, $\text{m}^3 \cdot \text{s}^{-1}$.

(5) Heat dissipation from the external surface of cell Q_{loss}

Q_{loss} is heat dissipation from the external surface of cell through convection and radiation. When there is no external wind effect of draught fan, or natural high wind, the convective heat transfer coefficient (α_{conv}) can be gained through free convection calculation formula (19)-(22) [11].

$$Pr = \frac{c_p \mu}{\lambda} \quad (19)$$

$$Gr = \frac{\beta g \Delta t l^3 \rho^2}{\mu^2} \quad (20)$$

$$Nu = C(Gr \cdot Pr)^n \quad (21)$$

$$\alpha_{\text{conv}} = \frac{Nu \lambda}{l} \quad (22)$$

Where, c_p , μ , λ and ρ are the specific heat, coefficient of viscosity, heat conductivity coefficient and density of air respectively. g is gravitational acceleration. Pr shows the ratio of viscous diffusion rate to thermal diffusion one, it can be obtained via formula (19) or directly consulting relevant reference books.

$\beta = \frac{1}{T} = \frac{1}{t_m + 273}$, t_m is average temperature of wall temperature (t_w) and environment air temperature (t). All the air properties used for above calculation are ones at t_m .

l is feature size of heat transfer surface, m. For side wall, l is the height of area, while for top and bottom surface, l is the area of surface divided by its perimeter.

C and n are influenced by the shape and location of heat transfer wall, temperature boundary conditions and air flow states. They could be determined by consulting experimental data.

The calculated convective heat transfer coefficients vary nonlinearly with wall temperatures. It is necessary to consider high wind effect from outside workshop for bottom shell and cradle.

The radiation heat transfer coefficient could be added into the thermal-electric model directly through radiation analysis model of ANSYS, or be equivalent to convective heat transfer coefficient and loaded into the model by SFA command. SFA command is used to specify surface loads on the selected areas and could also be realized by GUI operation of (Main Menu > Preprocessor > Loads > Define Loads > Apply > Thermal > Convection > On Areas). The radiant heat (Q_{rad}) is described as below.

$$Q_{\text{rad}} = \varepsilon \sigma_0 \varphi A (T_1^4 - T_2^4) \\ = \varepsilon \sigma_0 \varphi (T_1^2 + T_2^2) \times (T_1 + T_2) \times (T_1 - T_2)$$

$$= \varepsilon \sigma_0 \varphi (T_1^2 + T_2^2) \times (T_1 + T_2) \times A (T_1 - T_2) \quad (23)$$

Where, σ_0 is radiation constant of blackbody, $\sigma_0 = 5.669 \times 10^{-8} \text{ W} \cdot \text{m}^{-2} \cdot \text{K}^{-4}$; ε is emissivity, it is 0.8 for shell and cradle; φ is view factor, it is 1 for location only with radiation heat transfer between cell surface and environment; A is area of the heat transfer surface, m^2 ; T_1 and T_2 are wall temperature and environment temperature respectively, K.

Therefore, the equivalent convective heat transfer coefficient (α_{rad}) could be described as

$$\alpha_{\text{rad}} = \varepsilon \sigma_0 \varphi (T_1^2 + T_2^2) \times (T_1 + T_2) \quad (24)$$

Except radiant heat transfer between external wall and environment air, there are also radiative interactions between a position of a cell's external wall with another position, or between external walls of adjacent cells. Yang Shiming exhibits a series of calculation models in [11], α_{rad} for the special locations could be adjusted by relevant view factor (φ) calculations.

The integrated heat transfer coefficient (α) of convective and radiation is expressed as formula (25) and loaded to the calculation model by SFA command.

$$\alpha = \alpha_{\text{conv}} + \alpha_{\text{rad}} \quad (25)$$

Model description

A quarter 3D 305kA thermal-electric model of aluminium electrolysis cell for thermal balance calculation is established and shown as Figure 1. Two solid element types are employed, thermal-electric SOLID 69 for the current-carrying parts such as anode rod, anode steel claw, carbon anode, bath, molten metal, cathode and bar, and thermal SOLID 70 for other thermal insulating materials. The contact element CONTA173 and target element TARGE170 are also applied to achieve the electric and thermal contacts.

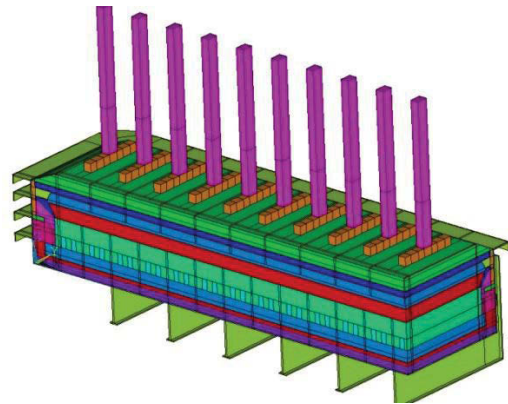


Fig.1 Geometrical model of quarter aluminium reduction cell

Material non-linearity is in consideration via definition of temperature dependent heat conductivity and electrical resistivity through ANSYS parametric design language. The thermal conductivity of the bath and metal is $1.69 \text{ W} \cdot \text{m}^{-1} \cdot \text{°C}^{-1}$ and $77.95 \text{ W} \cdot \text{m}^{-1} \cdot \text{°C}^{-1}$ respectively [12]. Owing to the complicated melt flowing, the temperature is almost uniform. To achieve this, huge thermal conductivity ($50000 \text{ W} \cdot \text{m}^{-1} \cdot \text{K}^{-1}$) for electrolyte

and for horizontal components of molten metal is defined while the vertical conductivity of metal is still $77.95 \text{ W} \cdot \text{m}^{-1} \cdot \text{°C}^{-1}$.

Electric and thermal contact

There is no-ignorable contact resistance between cathode carbon and bar [13]. Electric contact problems can be solved by equation (26). ANSYS software has the capacity of dealing with contact problems [14].

$$J = ECC \times (\phi_t - \phi_c) \quad (26)$$

Where, J is current density, $\text{A} \cdot \text{m}^{-2}$; ECC is electric contact conductance, Beeler R [13] and Li Jingjiang [15] showed that the electric contact resistance between cathode and paste was $1 \times 10^{-5} \Omega \cdot \text{m}^2$, and the one between paste and bar was $0.3 \times 10^{-5} \Omega \cdot \text{m}^2$. Consequently, the electric contact resistance between cathode and bar in the model is $1.3 \times 10^{-5} \Omega \cdot \text{m}^2$, then ECC is $0.77 \times 10^5 \text{ S} \cdot \text{m}^{-2}$; ϕ_t and ϕ_c are the potential of contact surfaces, V.

The counter EMF is made up of decomposition voltage and overvoltage. The voltage drop in gas layer and EMF can be described by electric contact definition. The equivalent ECC in the interface between bath and anode is worked out by formula (27).

$$ECC_{surf} = \frac{J_{surf}}{V_g + V_{dec} + V_p} \quad (27)$$

Where, ECC_{surf} is the equivalent ECC between bath and anode, $\text{S} \cdot \text{m}^{-2}$; J_{surf} is the interface current density, $\text{A} \cdot \text{m}^{-2}$; $V_g + V_{dec} + V_p$ comprises gas layer voltage drop, decomposition and polarization voltage, V.

The heat generated in bath and its interface with anode carbon is transferred out through top anodes, side ledge, and bottom cathodes by severe convection caused by high speed flowing of melt. The heat transfer through the interfaces can be described as

$$Q = h_E \cdot A_E \cdot (T_S - T_L) \quad (28)$$

Where, h_E is the heat convection coefficient of the melt to side boundaries, $\text{W} \cdot \text{m}^{-2} \cdot \text{°C}^{-1}$; A_E is the area of contact surface, m^2 ; T_S and T_L are the temperature of melt and boundary surface respectively, °C .

Thermal contact problems in ANSYS software is described as formula (29) [14].

$$q = TCC \times (t_t - t_c) \quad (29)$$

Where, q is the heat flux per area, $\text{W} \cdot \text{m}^{-2}$; t_t and t_c are the temperatures of the contact points on the target and contact surfaces respectively, °C ; TCC is the thermal contact conductance coefficient, it is equal to the heat convection coefficient h_E and has same unit, $\text{W} \cdot \text{m}^{-2} \cdot \text{°C}^{-1}$. Thus the convective heat transfer between melt and its adjacent anodes, frozen electrolyte, or cathodes could be described by thermal contact model provided by ANSYS software. The convective heat transfer coefficient is defined as TCC [16].

A series of KEYOPTs is available for element CONTACT173, and KEYOPT (1) is used to select degrees of freedom. For the case involving both current running and heat transfer, KEYOPT (1) =4 is set to define VOLT and TEMP degrees of freedom, at the same time, FHEG in the real constant of the contact pair is defined as 1 so as to consider Joule heat. Contact pairs between bath and anode, between molten metal and cathode, between cathode and bar are all such examples. On the interface between bath and anode, the Joule heat generated by gas film layer voltage and EMF is mainly on the side of electrolyte. Therefore FWGT is set as $1e-8$ to represent true 0. The input 0 is interpreted as the default value 0.5 by ANSYS.

For the case involving only heat transfer, KEYOPT (1) =2 is set to define TEMP degree of freedom. Contact pairs between melt and side ledge, between bar and bottom insulating materials are such examples.

Boundary conditions

Electrical boundary conditions are simple. The top nodes of anode rod are set with equal current and constrained as equipotential. The end areas of cathode collector bars act as zero potential place. The current flows through the whole cell and generates Joule heat correspondingly in rod, claw, anode carbon, the interface between anode and bath, bath, aluminium, cathode carbon, the interface between cathode and bar, and bar. The bath and its interface with anode is the main heat source of the cell.

The integrated heat transfer coefficients α in different locations of cell external walls obtained by (25) are applied correspondingly by SFA command. The heat transfer coefficient on the surface of anode cover is determined mainly by fume/gas flow rate under hood, therefore α in that location is valued empirically, $15 \text{ W} \cdot \text{m}^{-2} \cdot \text{K}^{-1}$ is set in this paper. Heat dissipation from the external surface of cell Q_{loss} could be realized by α definition and extracted by the final results.

Other energy expenditures are described in the model by negative heat generation rate definition through BFV command, which is used to define a body force load on a volume and could also be realized by GUI operation of (Main Menu > Preprocessor > Loads > Define Loads > Apply > Thermal > Heat Generat > On Volumes). The negative heat generation rate is calculated as formula (30) and thought to be distributed equally in the loaded volume.

$$q_n = \frac{-Q_n}{V_n} \quad (30)$$

Where, q_n is the negative heat generation rate, $\text{W} \cdot \text{m}^{-3}$; Q_n is heat expenditure, W; V_n is the volume of loaded volume body, m^3 ; n is the designation of different heat expenditures, for example, n is 'dec' for Q_{dec} . The loaded volume bodies for different energy expenditures are listed as below.

- (1) Energy for decomposition reaction Q_{dec} is applied on bath;
- (2) Energy taken away with removed liquid aluminium $Q_{alu}^{t_2-30}$ is applied on molten metal;
- (3) Heat losses caused by anode change Q_{and} is applied on anode carbon;

- (4) Energy taken away with fume/air gases Q_{gas} is applied on the air above electrolyte and electrolyte above anode bottom level.

The bath temperature 950°C is applied on nodes of bath initially. Through thermal-electric simulation and results analysis, whether heat balance is achieved could be checked out. If requirements are not met, the insulation construction is changed, the model is rebuilt and calculation is repeated, until the cell structure reaches heat equilibrium. After that, the node temperature constraints are deleted, and the final temperature profile of cell is recalculated, so as to verify its rationality.

Results and discussion

An existing 305kA aluminum reduction cell structure is chosen for the thermal balance calculation. Hence the insulation construction is already determined. Many parameters of boundary conditions are obtained by actual measurements. Initially, bath temperature is constrained as 950°C. With some anode cover height adjustments, the heat balanced results are obtained. Figure 2 shows the final potential distribution of the cell.

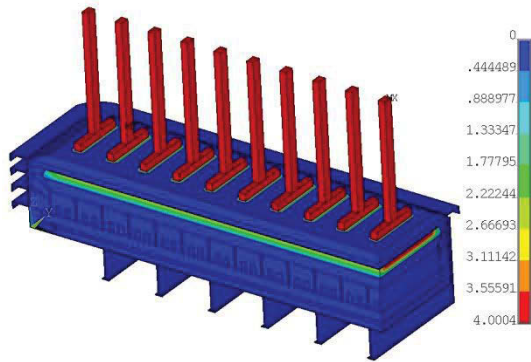


Fig.2 Potential distribution of the cell/V

The results show that the cell voltage is 4.0004 V. Besides ohmic voltage drop, EMF and gas film layer voltage drop are well expressed in thermal-electric modeling by the definition of electrical contact pairs. The calculated electric balance and practical measurements are listed together in Table 1.

Tab.1 Electrical balance of calculated value and practical measurements /mV

Item	Calculated value	measurements
Anode group	241.9	354.2
EMF	1550	1550
Gas film voltage drop	348.9	-
Bath	1542.2	1724.4
Molten metal	0.3	-
Cathode	317.1	405.5
Cell voltage	4000.4	4033.6

In calculation, EMF and gas film voltage are together described as contact voltage drop between bath and carbon anodes, their sum is 1898.0 mV. The measurements only got EMF as 1550mV and gas film voltage drop cannot be measured. It is supposed that gas film voltage drop is allocated to anode group and bath in measurements. That is why the calculated voltage drops of anode group and bath are less than measured ones.

In most of prebaked smelters, there are undissolved alumina, pieces of broken carbon anode, and some broken top crust over the cathode blocks. They inevitably increase the cathode voltage drop. However, their influence cannot be estimated properly and be modeled quantitatively in calculation. That is reason why measured cathode voltage drop is 90 mV higher than calculated one. Measured CVD of another cell with same cell structure and series amperage, is 316.2 mV, same with calculation.

Figure 3 presents temperature profile of the cell with bath temperature constraints. Owing to calculation errors on the interfaces with contact definition, the maximum temperature is 951.6°C, higher than predefined molten temperature 950°C. The small calculation error does not affect thermal balance results and is ignored.

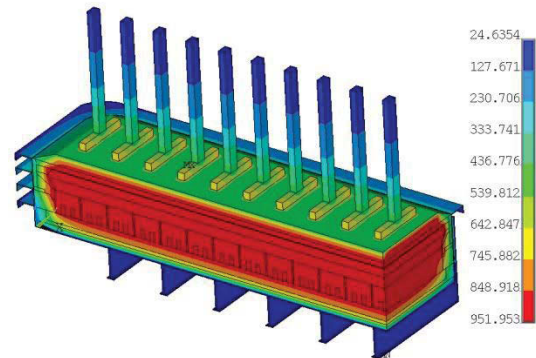


Fig.3 Temperature profile of the cell with bath temperature constraints/°C

Figure 4 shows the temperature profile of bath and aluminium. Gradient presents in vertical direction of aluminium. That is in agreement with practical situation. The temperature difference between aluminium top and bottom is about 4°C~7°C.

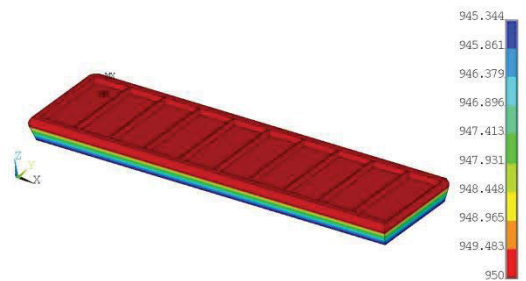


Fig.4 Temperature field of molten bath and liquid aluminium

Table 2 presents the energy balance of the cell obtained by analysis of calculation results. The workshop temperature is the base temperature. All the energy expenditures except heat losses from external surfaces are obtained by theoretical calculation using former introduced formula with reference of related notebooks and practical measurements.

The imbalance between energy input and energy expenditure are 4kW, about 0.39%, so it is concluded that the cell has good thermal balance.

Apart from the generated high temperature CO_2/CO , under the action of cell ventilation, cool air from around the cell enters into

space under cell hoods, then is heated up and finally extracted together with CO₂/CO out of the cell to surrounding atmosphere. As a result, Q_{gas} occupies large proportion of the energy expenditure, about 43.07%. The fume extraction rate which has strong impact on duct gas temperature and cell emission is of great importance for the cell balance.

Tab.2 Energy balance of aluminium reduction cell

items		kw	V	%
Energy input	Energy power supply A_{ele}	1233.8	4.0454	100
	Raw material enthalpy A_{mat}	0	0	0
	Total energy income A_{total}	1220.8	4.0004	100
Energy expenditure	Decomposition reaction Q_{dec}	529.8	1.737	43.26
	Removed metal enthalpy Q_{alu}	34.6	0.1134	2.82
	Spent anode enthalpy Q_{and}	9.6	0.0315	0.78
	Extracted fume/air gases Q_{gas}	256.0	0.8393	20.90
	Heat losses from surfaces Q_{loss}	394.8	1.2944	32.23
	<i>Heat losses from top</i>	114.6	0.3757	9.36
	<i>Heat losses from side and end</i>	242.4	0.7948	19.79
	<i>Heat losses from bottom</i>	37.8	0.1239	3.09
	Total energy expenditure Q_{total}	1224.8	4.0156	100
	Imbalance	4	0.0152	0.39

The thermal-electric model is recalculated when the temperature DOFs of bath nodes are deleted, the retrieved bath temperature is 949°C. The potential and temperature distribution is similar to former ones. All of these further verify the reasonability of the thermal balance calculation method.

Conclusions

An improved quarter 3D thermal-electric model of aluminium reduction cell is developed by commercial software ANSYS in order to evaluate the cell's thermal balance. Temperature dependent material properties of thermal conductivity and electrical resistivity, as well as integrated convective heat transfer coefficient on the external surface, are considered in the model through ANSYS parametric design language.

Contact pairs are introduced to the thermal-electric model. Thermal contacts are used to well describe internal convective heat transfers between melt and its adjacent anodes, sideledge and cathodes, with convective heat transfer coefficient acting as TCC. Electrical contact pairs are applied on interface between cathodes and bars to model the contact resistance. It is also present between anode and molten electrolyte to state the EMF and gas film layer resistance. For the electric contact pairs, the FHEG is set as 1 to take Joule heat into account.

Taking the workshop temperature as base temperature, by theoretical calculations consulting previous measurements and related notebooks, the energy for decomposition reaction and heat losses caused by taping, anode change and fume/air extraction are obtained and loaded into simulation.

Taking an existing 305kA aluminium reduction cell as calculation example, the results show that the total calculated cell voltage has little difference with measured one. The total energy input is 4kW less than energy expenditure, which shows the cell is well thermal balanced. All these demonstrate that the thermal balance calculation method of aluminium reduction cell is rational.

References

1. László I. Kiss, Véronique Dassylva-Raymond. FREEZE THICKNESS IN THE ALUMINUM ELECTROLYSIS CELLS. Light Metals (2008), 431-436
2. Li jie, Wang Zhigang, Cell profile and heat balance of 5kA inert anode aluminum reduction cells. The Chinese journal of process engineering. 2008, 8(SUPPL), 54-58.
3. Cui Xifeng, Zou Zhong. Simulation calculation of 3D freeze profile in prebaked aluminum reduction cells. Journal of Central South University, 2012, 43(3), 815-820
4. Gennady V. Arkhipov, Vitaly V. Pingin, Yaroslav A. Tretyakov, Peter V. Polyakov. SIMULATION OF CELL THERMOELECTRIC FIELD WITH CONSIDERATION OF ELECTRO CHEMICAL PROCESSES. Light Metals (2007), 327-331
5. Sophie Poizeau, Donald R. Sadoway. Towards a design tool for self-heated cells producing liquid metal by electrolysis. Light Metals (2011), 387-392
6. Dupuis M. Computation of aluminum reduction cell energy balance using ANSYS finite element models. Light Metals (1998), 409-417
7. Vanderlei Gusberti, Dagoberto S. Severo, Barry J. Welch, Maria Skyllas-Kazacos. MODELING THE MASS AND ENERGY BALANCE OF DIFFERENT ALUMINIUM SMELTING CELL TECHNOLOGIES. Light Metals (2012), 929-934
8. Haupin W E. Calculating thickness of containing walls frozen from melt. Light Metals (1971), 188-194
9. Kryukovsky V A, Scherbinin S A. Mathematical modeling of heat transfer in pots lining materials for production of non-ferrous metals. Light Metal (1991), 557-562
10. Bruggeman J N, Danka D J. Two-dimensional thermal modeling of the Hall-Héroult cell. Light Metals (1990), 203-209
11. Yang Shiming, Tao Wenquan. Heat Transfer. (Beijing: Higher Education Press, 2007), 263-279
12. Ai D K. The hydrodynamics of the hall-heroult cell. Light Metals (1985), 593: 607.
13. Beeler R. An analytical model for cathode voltage drop in aluminum reduction cells. Light Metals (2003), 241-245
14. ANSYS Inc. Theory Reference, Chapter 7 Metaphysics Contact.
15. Li Jingjiang, Qiu Zhuxian. 3-D numerical calculation and analysis of electric field for the cathode of aluminum reduction cells. Journal of Northeast University of Technology, 1989, 10(6), 591-597
16. Cui Xifeng, Zhang Hongliang, et al. 3D Freeze Shape Study of the Aluminum Electrolysis Cells Using Finite Element Method. Light metals (2010), 447-452